Dynamics of Drift and Flute Modes in Linear Cylindrical ECR Plasma

Kunihiro KAMATAKI [1)], Sanae –I. ITOH[2)], Yoshihiko NAGASHIMA[3)], Shigeru INAGAKI[2)], Shunjiro SHINOHARA[1)], Masatoshi YAGI[2)], Takuma YAMADA[3)], Yoshinobu KAWAI[1)], Akihide FUJISAWA[4)], and Kimitaka ITOH[4)]

[1)] *Interdisciplinary Graduate School of Engineering Science, Kyushu University, Kasuga, Fukuoka 816-8580, Japan*
[2)] *Research Institute for Applied Mechanics, Kyushu University, Kasuga, Fukuoka 816-8580, Japan*
[3)] *Graduate School of Frontier Sciences, The University of Tokyo, Kashiwa, Chiba 277-8561, Japan*
[4)] *National Institute for Fusion Science, Toki, Gifu 509-5292, Japan*

(Received: 17 September 2008 / Accepted: 10 December 2008)

Competitive and coexistence phenomena of a drift mode and a flute mode have been observed experimentally in linear cylindrical electron cyclotron resonance (ECR) plasmas. The drift mode is dominant in the low neutral gas pressure. The flute mode is excited and become dominant with the increase in the neutral gas pressure. The coexistence of the drift and flute modes is observed in the intermediate neutral gas pressure regime. The radial profiles of density, its gradient scale length and floating potential are different in the each regime. In the coexistence regime, the drift mode and the flute mode appear alternately in a single discharge. This competition is related to the rise and the crash of the density and its gradient, and the crash occurs inside and outside of this plasma at the same time, and density increases simultaneously outside when the density decrease abruptly in the central plasma region.

Keywords: competition, coexistence, crash, drift mode, flute mode, and linear cylindrical ECR plasma

1. Introduction

The nonlinear self-regulation mechanism of drift wave turbulence has been subject to attention in order to show the structural formation of plasma turbulence [1-2]. The plasma transport across the magnetic field is strongly affected by low frequency (much lower than the ion cyclotron frequency) fluctuations, e.g. the drift wave instability. In addition, the multi-scale interaction between dissipative instabilities and reactive instabilities has attracted attentions in the magnetic confinement devices [3]. The collisional drift mode is dissipative and the flute mode is reactive. The coupling between dissipative and reactive instabilities has attracted attention in studies of the magnetic confinement devices [4]. The drift wave is well known as a universal low frequency instability driven by the free energy provided by a pressure gradient transverse to the magnetic field [5]. In mirror machines, the averaged magnetic curvature is responsible for an effective gravity, which allows the flute instability to develop. Several studies [6-8] on the drift and the flute (interchange) modes have been reported. However, the coupling of the drift and the flute modes has not been clarified yet.

We have already observed the coexistence of the collisional drift mode and the flute mode in linear cylindrical ECR plasma [9]. Studies of the coexistence phenomena are expected to clarify the dynamics between the drift mode and flute mode, and to understand comprehensively the multi-scale turbulence. In this article we report the dynamics of the drift mode and the flute mode, focusing on the competitive and the coexistence phenomena.

2. Experimental setup

The experiments have been performed on a linear cylindrical ECR plasma device [9]. The cylindrical vacuum chamber consists of stainless steel with the inner diameter is 40 cm and the axial length is 120 cm. Argon gas is fed into the vacuum chamber using a mass flow controller. The chamber is evacuated to a base pressure less than 10^{-7} Torr using a rotary pump and a 1000 1/s turbo molecular pump [working pressure is $p_{(\mathrm{Ar})}$ = (0.2 - 2.0) mTorr]. Eight magnetic coils (axial width is 6.4 cm in z-direction and outer diameter is 71.5 cm) form a mirror magnetic field configuration. Microwave with the frequency of 2.45 GHz and the output power P_{μ} = 300W is launched into a chamber through the coaxial waveguide converter (inner diameter is 10 cm and axial length is 21 cm). The reflected power is reduced by a three-stub tuner and a movable metal plate in the coaxial waveguide. The axial boundary condition is determined from both ends of the vacuum chamber (terminated by metal flanges).

The plasma fluctuations (ion saturation current I_{is} and floating potential V_{f}) are measured with the Langmuir probes (a tungsten tip with 1mm in diameter and 2 mm in length). Time traces of I_{is} and V_{f} signals are recorded by a data logger with a sampling rate of 1 MHz (16 bit). The

author's e-mail: kamataki@riam.kyushu-u.ac.jp

Langumuir probes are set at eight azimuthal positions and five axial positions. The azimuthal mode number m and the parallel wave number n can be determined from these measurements. Here, n = 1 indicates that the half wavelength is the same as the device length. In order to measure the spatio-temporal structures of modes, we have developed a multi-channel Langmuir probe array. The array has stainless-steel rings (outer diameter of 3 mm, inner diameter of 2.5 mm and length of 1.2 mm) positioned in the radial direction (with the radial separation of 10 mm), which are based on an alumina tube (outer diameter of 2 mm, inner diameter of 1.5 mm and length of 200 mm). The same type of probe array in a toroidal plasma device is in Ref. [10]. The time-averaged and the fluctuated radial density gradient are determined from this probe array. Typical plasma parameters are as follows: electron density $n_e \sim 10^{11}$ cm^{-3} and electron temperature $T_e \sim 2$ eV under the typical discharge condition (the measurement point of z = 30 cm and r = 3 cm with magnetic field strength B = 685 Gauss). These are obtained from current-voltage (*I-V*) characteristics of the Langumuir probe.

3. Experimental results

In this linear plasma, both of the drift mode and the flute mode are excited in a particular neutral pressure region [9]. The two modes [the drift mode (m/n = 4/1) and the flute mode (m/n = 2/0)] were identified from the measurement of the axial and the azimuthal wave numbers, phase differences between density and potential fluctuations, and the comparison between normalized amplitudes of density and potential fluctuations. Figure 1 (quoted from Ref. [11]) shows the amplitude of both modes as a function of the neutral gas pressure, which is used as an index of the collisional damping of each mode. In the lower filling gas pressure regime $p_{(Ar)}$ = (0.2 – 0.6) mTorr (state 1), the drift mode is excited but the flute mode is stabilized. In the higher pressure regime $p_{(Ar)}$ = (1.6 – 2.0) mTorr (state 3), the flute mode is excited and only the drift mode is stabilized. In an intermediate regime $p_{(Ar)}$ = (0.6 – 1.6) mTorr (state 2), the drift mode is gradually suppressed and the flute mode becomes unstable and thus the two modes are coexistent. A linear stability analysis using the Hasegawa-Wakatani model [12] gives similar growth rates of two modes in this coexistence condition [9]. The state 2 is considered to be a middle-state for a smooth transition from the state 1 to the state 3. Figure 2 shows the radial profiles of I_{is}, inverse scale length of density gradient $\nabla n/n$ and V_f in the each of states [the state 1 ($p_{(Ar)}$ = (0.2 and 0.4) mTorr), the state 2 ($p_{(Ar)}$ = (0.8, 1.0, 1.2 and 1.4) mTorr), and the state 3 ($p_{(Ar)}$ = (1.8 and 2.0) mTorr)]. Figures 2 (a), 2 (b), and 2 (c) show that I_{is} has peaked radial profiles in each of states.

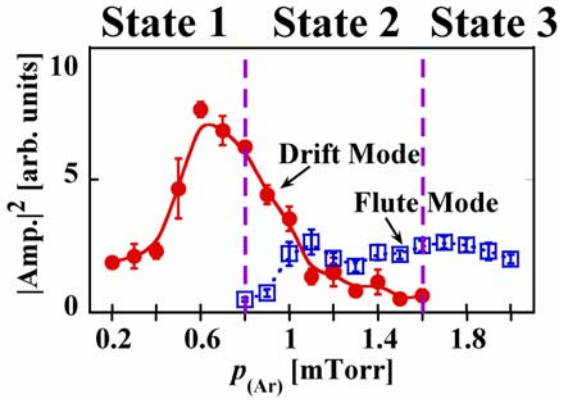

Fig. 1 Dependence of square of drift and flute modes fluctuations amplitude on the neutral gas pressure including the line to divide operation regions into states 1-3. (quoted from Ref. [11])

The I_{is} at the center increases with the increase in the neutral gas pressure (from the state 1 to the state 3). The radial profiles of $\nabla n/n$ in each state are shown in Figs. 2 (d), 2 (e), and 2 (f). In the state 1, the $\nabla n/n$ is peaked at r = 4 cm, where the drift mode has maximum amplitude (not shown). The $\nabla n/n$ is peaked at r = 3 cm, where the drift mode and the flute mode have the largest amplitudes (not shown) in the state 2. Moreover, the peak value of $\nabla n/n$ increases as the neutral gas pressure increase in the state 1 and 2. The radial position of peak $\nabla n/n$ is r = 3 – 5 cm where the flute mode is excited most strongly (not shown). The radial profiles of $\nabla n/n$ are corresponding to the excitations of both modes. The radial profiles of V_f in each state are shown in Figs. 2 (g), 2 (h), and 2 (i). The radial profile of V_f is flat at r > 4 cm and decreases strongly toward the plasma center at $p_{(Ar)}$ = 0.4 mTorr in the state 1. The radial profile of V_f are almost same while that of I_{is} changes at $p_{(Ar)}$ = 1.0 – 1.4 mTorr in state 2. The V_f at the center increases from ~ -25 V to ~ -5V as the neutral gas pressure increases from state 1 to state 2. At $p_{(Ar)}$ = 2.0 mTorr (in the state 3), that of V_f remain relatively flat at all radial positions. The space potential V_s is calculated from the equation $V_s = V_f + \alpha T_e$ (α is the constant). The ion saturation current I_{is} is proportional to $n_e T_e^{1/2}$. The radial profile of T_e remains relatively flat at $p_{(Ar)}$ = 1.0 mTorr [9]. It is assumed that that of T_e is flat in these experiments, which leads $\nabla V_f \sim \nabla V_s$ and $\nabla I_{is}/I_{is} \sim \nabla n/n$, and the influence of electron temperature fluctuations is negligible. The qualitative features of dynamics of two modes discussed in this paper are not affected by these assumptions. The measurement of the full radial profile of T_e is left for the future work. Moreover, the results in Figs. 2(a) - 2(c) indicate that the amplitudes of both n_e and T_e change with the increment of the neutral gas pressure. Therefore, the profile of V_s may change drastically with the increment of neutral gas

pressure, similar to that of V_f. It is found that the radial profiles of typical plasma parameters in each state have different features, which indicates that the drastic change of the radial profiles is related to the change of the dominant mode.

Figures 1 and 2 showed the features of the time averaged phenomena. In order to clarify the dynamics between the drift mode and the flute mode, we focus on the temporal behavior of both modes. In fact, the state 2 is a non stationary state. Figures 3 (a), 3 (b), and 3 (c) show the typical time evolutions of I_{is} and the equilibrium quantity I_{is0} (red lines) (using a low pass filter $f < 100$ Hz) in each of states. The fluctuation levels of I_{is} and I_{is0} in the state 1 and the state 3 are almost constant with time. On the other hand, I_{is} and I_{is0} repeated the rise and the drop at a certain period in the state 2. Time evolutions of density gradient ∇n_{e0} are similar to I_{is0} in each of states (shown in Figs. 3 (d), 3 (c), and 3 (e)). This repetition of I_{is0} and ∇n_{e0} indicates that a relaxation of global parameter takes place. The envelope analysis of each mode is useful to discuss the dynamics of waves. The envelopes of the fluctuation intensity in each of states, which are the drift mode and/or the flute mode measured using the band-pass filter, are shown in Figs. 3 (g), 3 (h) and 3 (i). Env. D (F) indicates the amplitude of the drift (flute) mode calculated from the envelope analysis. In the states 1 and 3, the drift mode and the flute mode stay with high amplitudes with time. In the state 2, it is found that there are two phases for one period in the coexistent modes: The state 2 is divided into the phase A and the phase B, as indicated by the vertical dashed lines. The amplitude of the drift mode is larger than that of flute mode in the phase A. On the other hand, the amplitude of flute mode is larger than that of drift mode in the phase B. It is found that the change of the dominant mode is observed between the phase A and phase B. In the phase A, the drift mode stays with higher amplitude with the smaller amplitude of the flute mode and I_{is} and ∇n_{e0} grow slowly. When the I_{is} and ∇n_{e0} exceed a critical value, the amplitude of the flute mode begins to increase suddenly (phase B). The amplitude of the drift mode decreases as that of the flute mode increases. Finally, when the I_{is} and ∇n_{e0} reach a limit at the end of the phase B, the 'crash' (the rapid drop) of I_{is} and ∇n_{e0} take place and it leads to the decrease (increase) of the flute (drift) mode and the phase A starts again. The coexistent state of the drift and the flute modes is realized by a competitive oscillation between them. The transition of each mode may be coupled.

The phenomena of the 'crash' appear in only the state 2. Finally, the characteristics of the crash are illustrated. The rise and the crash of I_{is} and ∇n_e with a certain period begin abruptly as the flute mode begins to be excited among the state 1 and the state 2, and finished as the drift mode is suppressed among the state 2 and the state 3. This

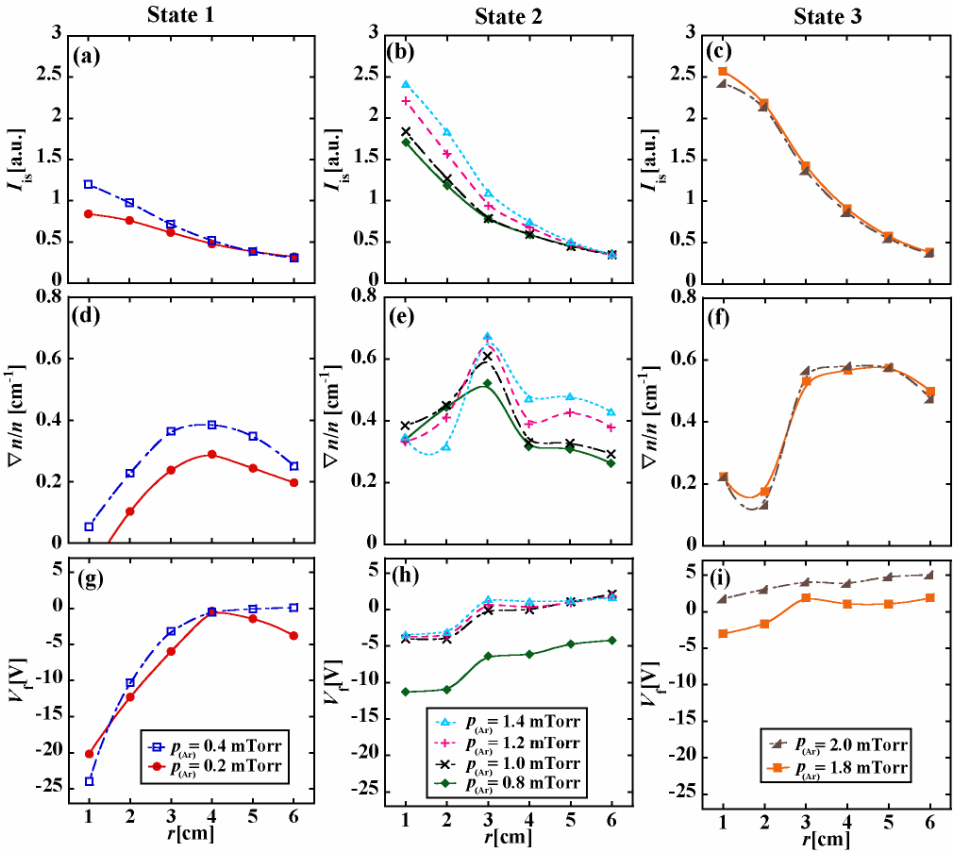

Fig. 2 Radial profiles of (a)-(c) the density, (d)-(f) its gradient inverse scale length, and (g)-(i) the floating potential in the each of states. [The state 1 ($p_{(Ar)}$ = (0.2 and 0.4) mTorr), the state 2 ($p_{(Ar)}$ = (0.8, 1.0, 1.2 and 1.4) mTorr), and the state 3 ($p_{(Ar)}$ = (1.8 and 2.0) mTorr)]

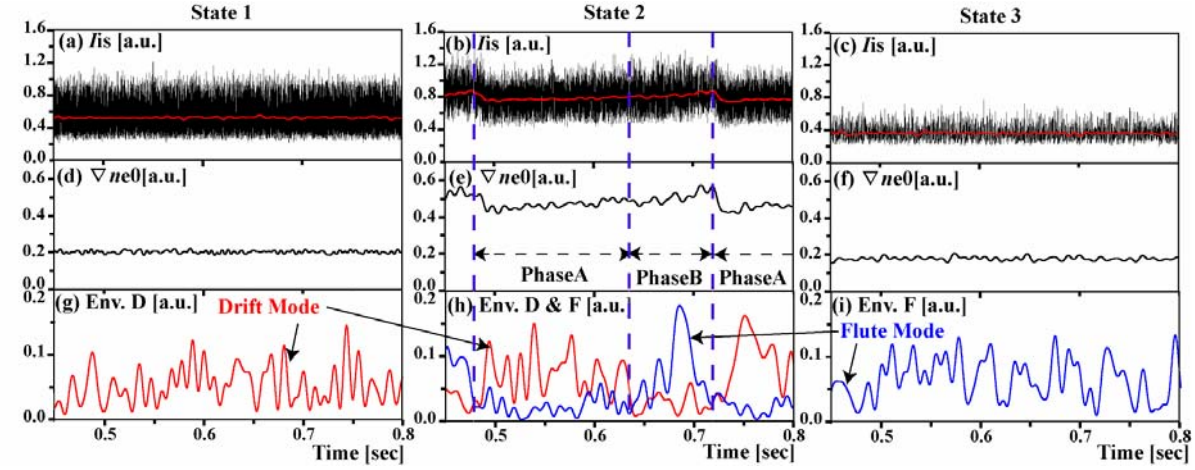

Fig. 3 Time evolutions of I_{is} in (a) the state 1, (b) the state 2, and (c) the state 3, an equilibrium quantity ∇n_{e0} in (d) the state 1, (e) the state 2, and (f) the state 3, envelopes (Env.) of (g) the drift (D) mode in the state 1, (h) the drift and flute (F) modes in the state 2 and (i) the flute mode in the state 3 at r = 4 cm (state 1), 3 cm (state 2), and 6 cm (state 3), where the amplitudes of the drift mode and/or flute mode at each of states peak.

result suggests the repetitions of I_{is} and ∇n_e are related to the competition of both modes. Figure 4 (a) and 4(b) show time evolutions of I_{is0} at r = 5cm (inside) and r =12 cm (outside) at $p_{(Ar)}$ = 0.8 mTorr (the state 2), respectively. Here, ΔT and ΔA indicate the interval time from the crash to the next one and the change of the amplitude of I_{is0} before and after the crash, respectively. The comparison of the radial profiles of I_{is} before and after the crash is shown in Fig. 4 (c). The simultaneous measurement of the crash at different radial positions shows the sudden break of density occurs at the same time inside and outside of this plasma, and when the density decrease abruptly in the central region (r < 9 cm), it increases simultaneously outside (r >10 cm). The ΔT at the central plasma (r = 0 cm) is the largest in the all radial positions. Figures 4 (d) and 4 (e) show the dependence on the ΔT and the relative amplitude $\Delta A/\langle I_{is}\rangle$ on the neutral gas pressure at r = 0 cm in the state 2, respectively. Here, $\langle\rangle$ is the temporal average. The ΔT increases slowly from as the neutral gas pressure increase ($p_{(Ar)}$ = (0.8 – 1.4) mTorr). After that gas pressure region, the ΔT increases strongly and can't be measured around $p_{(Ar)}$ ~ 1.6 mTorr. The discharge period is 1s. The $\Delta A/\langle I_{is}\rangle$ increases from ~ 20 % to ~ 30 % as the pressure increases. At $p_{(Ar)}$ > 1.1mTorr, the flute mode is larger than the drift mode (as shown in Fig. 1) These results indicate the relative strength of the drift and flute modes may be related to the characteristics of the crash in the coexistence state, which is left for the future work.

4. Conclusion

In conclusion, we have investigated the dynamics of the drift mode and the flute mode through the state 1 to the state 3 observed in the linear cylindrical ECR plasma. The radial profiles in each profile are different respectively, which indicates that the changes of the radial profiles are related to the changes of the dominant modes. The state 2 is considered to be a middle-state for a smooth transition

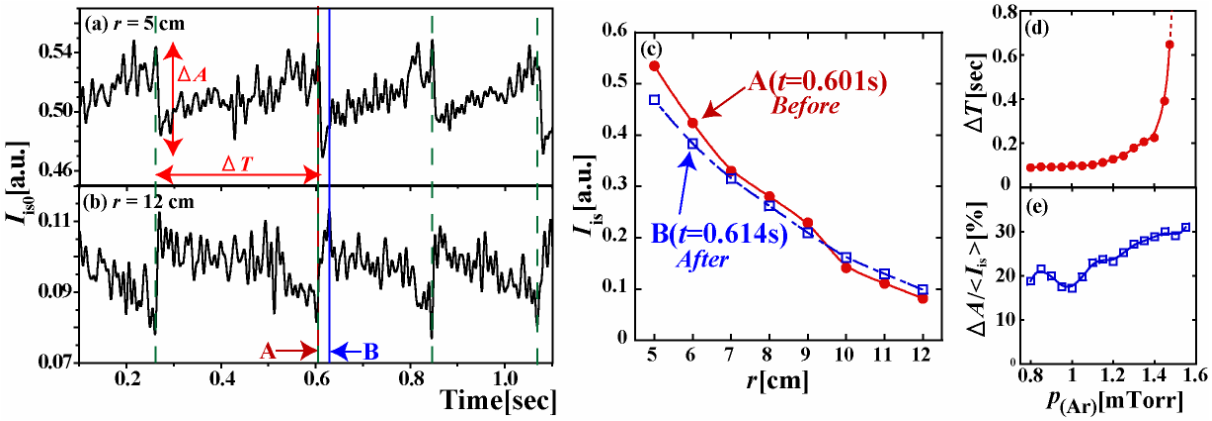

Fig.4 Time evolutions of I_{is0} at (a) r = 5cm (inside) and (b) r =12 cm (outside) at p(Ar) = 0.8 mTorr. (state 2). (c) Comparison of typical radial profiles of I_{is} before and after crash in Fig.4 (a). Crash starts at (A) t = 0.601s and ends at (B) t = 0.614.Vertical dash lines show start of crash. Here, ΔT and ΔA are illustrated in text. Dependence on (d) ΔT and (e) relative amplitude ΔA on the neutral gas pressure at r = 0 cm in state 2.

from the state 1 to the state 3. The coexistent state of the drift and the flute modes is realized by a competitive oscillation between them. The rise and the drop (the crash) of I_{is} and ∇n_e with a certain period appear in only coexistence state. It is found that the sudden break of density occurs at the same time inside and outside of this plasma, and density increases simultaneously outside when the density decrease abruptly in the central plasma region.

Acknowledgements

We would like to acknowledge useful discussions with Dr. A. Fukuyama, Dr. N. Kasuya, and Dr. S. Nishimura. This work is partly supported by a Grant-in-Aid for Specially-Promoted Research of MEXT of Japan (16002005), by Research Fellowships of the Japan Society for the Promotion of Science for Young Scientists, and by a collaborative program between the Research Institute for Applied Mechanics of Kyushu University and The National Institute for Fusion Science (NIFS) (NIFS07KOAP017).

[1] P. H. Diamond, S. –I. Itoh, K. Itoh, and T. S. Hahm, Plasma Phys. Control. Fusion **47,** R35 (2005).
[2] K. Itoh, S. -I. Itoh and A. Fukuyama, *Transport and Structural Formation in Plasmas* (IOP, Bristol, 1999).
[3] B. B. Kadomtsev and O. P. Pogutse: *Reviews of Plasma Physics* Vol.5 (Consultants Bureau, New York, 1970) p. 249.
[4] B. D. Scott, Phys. Plasma **12,** 62314 (2005).
[5] W. Horton, Rev. Mod. Phys. **71,** 735 (1999).
[6] A. Komori, N. Sato and Y. Hatta, Phys. Rev. Lett. **40,** 768 (1978).
[7] F. M. Poli *et al.,* Phys. Plasma **13,** 102104 (2006).
[8] J. C. Perez *et al.,* Phys. Plasma **13,** 32101 (2006).
[9] K. Kamatak *et al*., J. Phys. Soc. Jpn. **76,** 054501 (2007).
[10] S. H. Muller *et al*., Phys. Plasma **12,** 090906 (2005).
[11] K. Kamataki *et al*., Plasma Phys. Control. Fusion **50,** 035011 (2008).
[12] A. Hasegawa, and M. Wakatani, Phys. Rev. Lett. **59,** 1581 (1987).